Supplementary Materials: *N*-acetylglucosamine 2-Epimerase from *Pedobacter heparinus*: First Experimental Evidence of a Deprotonation/Reprotonation Mechanism

Su-Yan Wang, Pedro Laborda, Ai-Min Lu, Xu-Chu Duan, Hong-Yu Ma, Li Liu and Josef Voglmeir

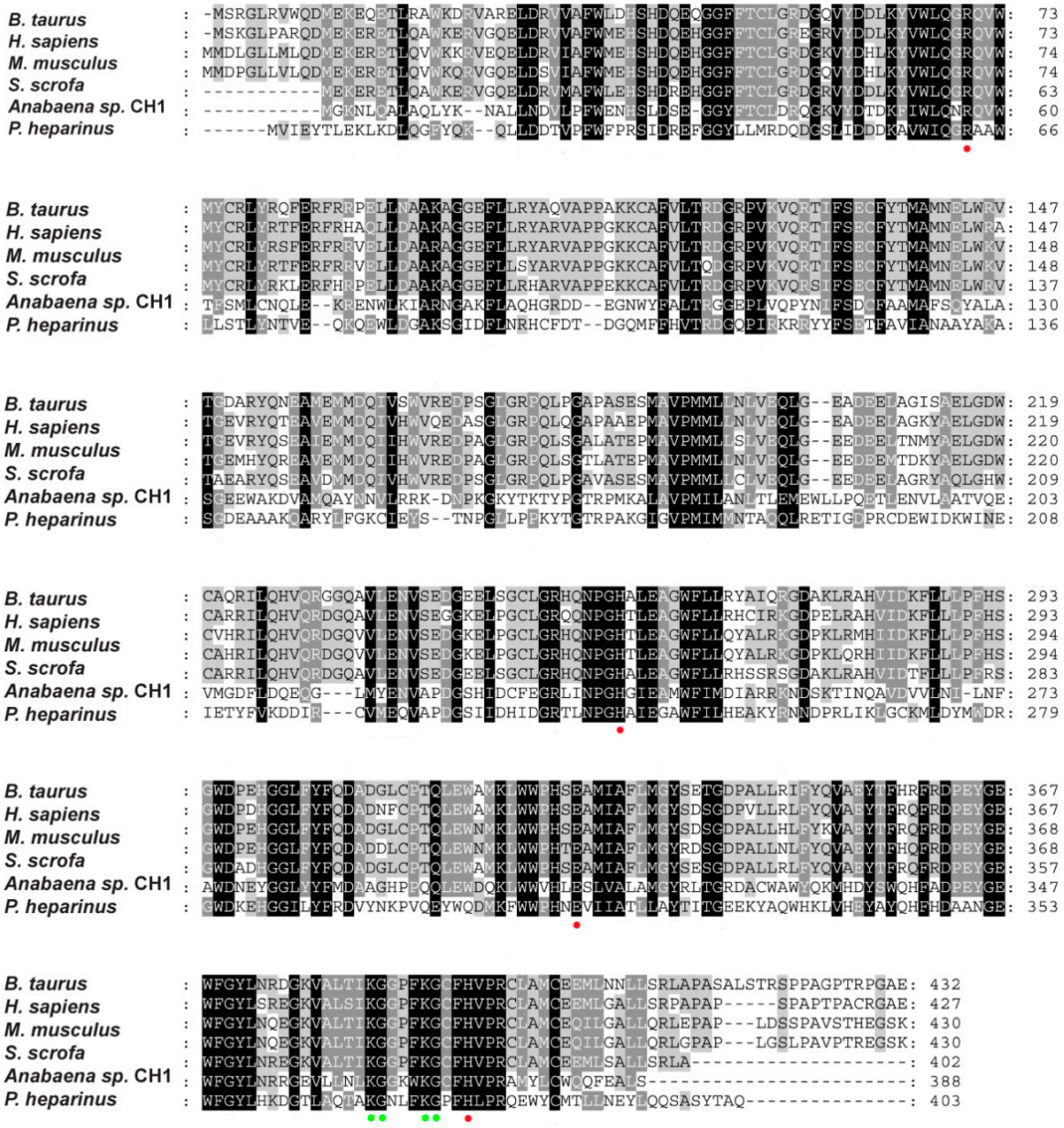

Figure S1. Amino acids sequence alignment of mammalian GlcNAc 2-epimerases from *Bos taurus*, *Homo sapiens*, *Mus musculus*, and *Sus scrofa*, bacterial GlcNAc 2-epimerases from *Anabaena* sp. CH1 and *Pedobacter heparinus*. Arg63, His244, Glu314 and His378 residues of *P. heparinus* epimerase, which are involved in the deprotonation/protonation steps, are indicated with a red spot. Lys369, Gly370, Lys374 and Gly375 residues of *P. heparinus* epimerase, which are involved in the ATP-binding process, are indicated with a green spot.

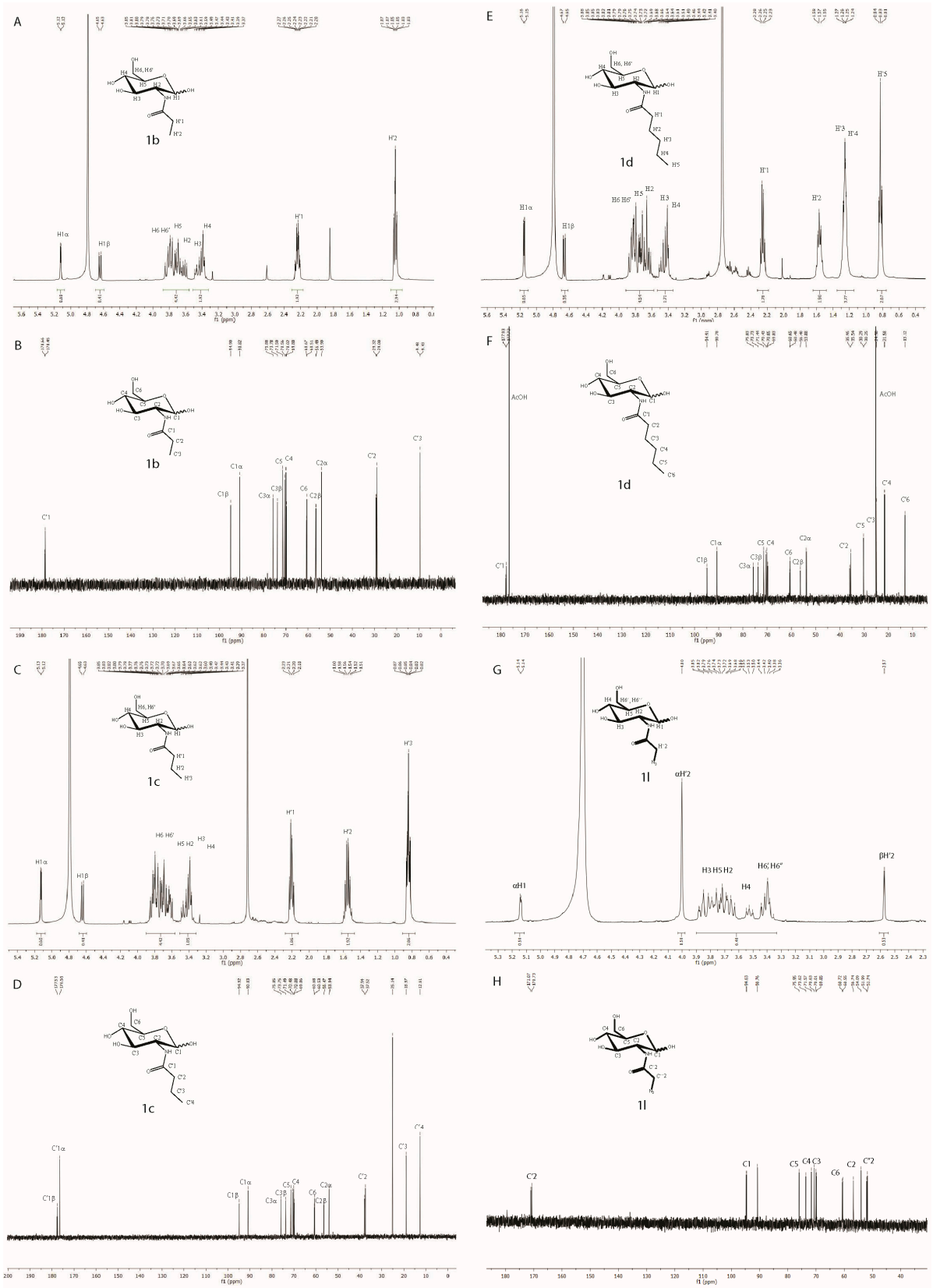

Figure S2. NMR characterization of GlcNAc analogues. (**A**) 1H of compound **1b**. (**B**) 13C of compound **1b**. (**C**) 1H of compound **1c**. (**D**) 13C of compound **1c**. (**E**) 1H of compound **1d**. (**F**) 13C of compound **1d**. (**G**) 1H of compound **1l**. (**H**) 13C of compound **1l**.

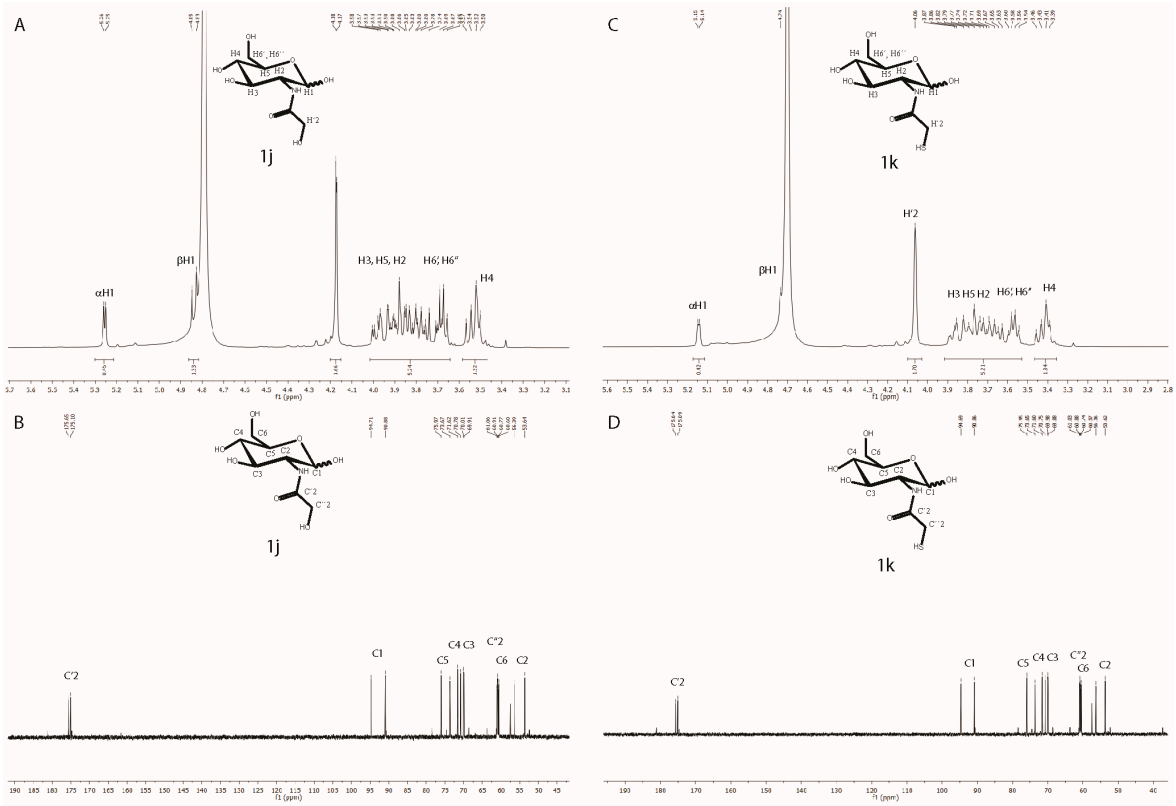

Figure S3. NMR characterization of GlcNAc analogues. (**A**) 1H of compound **1j**. (**B**) 13C of compound **1j**. (**C**) 1H of compound **1k**. (**D**) 13C of compound **1k**.

Table S1. The protein band on SDS-PAGE lane 4 was recovered and digested by trypsin. The digested solution was analyzed by MALDI-TOF MS and verified that the analyzed protein band is PhGn2E.

Observed Mr	Start-End	Peptide
2932.3590	337-360	LVHEYAYQHFHDAANGEWFGYLHK
2731.4129	308-330	FWWPHNEVIIATLLAYTITGEEK
2104.0974	239-257	TLNPGHAIEGAWFILHEAK
2054.9633	220-238	CVMEQVAPDGSIIDHIDGR
1942.9003	293-307	DVYNKPVQEYWQDMK
1928.9428	119-135	YYFSETFAVIANAAYAK
1759.9016	175-190	GIGVPMIMMNTAQQLR
1633.8373	20-32	QLLDDTVPFWFPR
1129.4805	272-279	MLDYMWDR
1091.5632	284-292	EHGGILYFR
1085.5448	37-45	EFGGYLLMR
921.4788	87-94	SGIDFLNR
823.4573	375-381	GPFHLPR

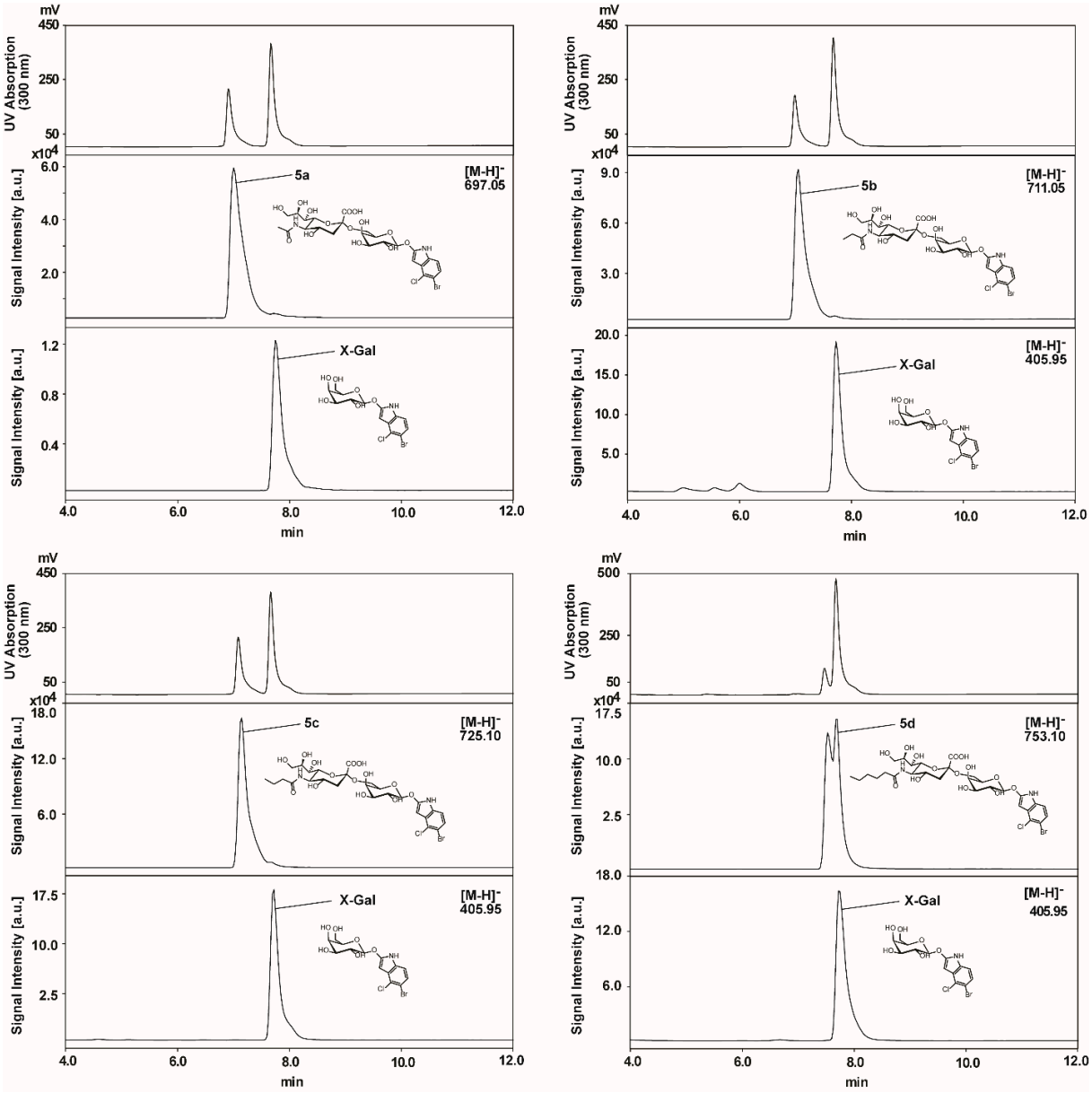

Figure S4. MS analysis of the Neu5Acα2-6GalβX analogues, **5a–d**, obtained by a four-enzyme, one-pot reaction using GlcNAc derivatives **1a–d** as the substrates.

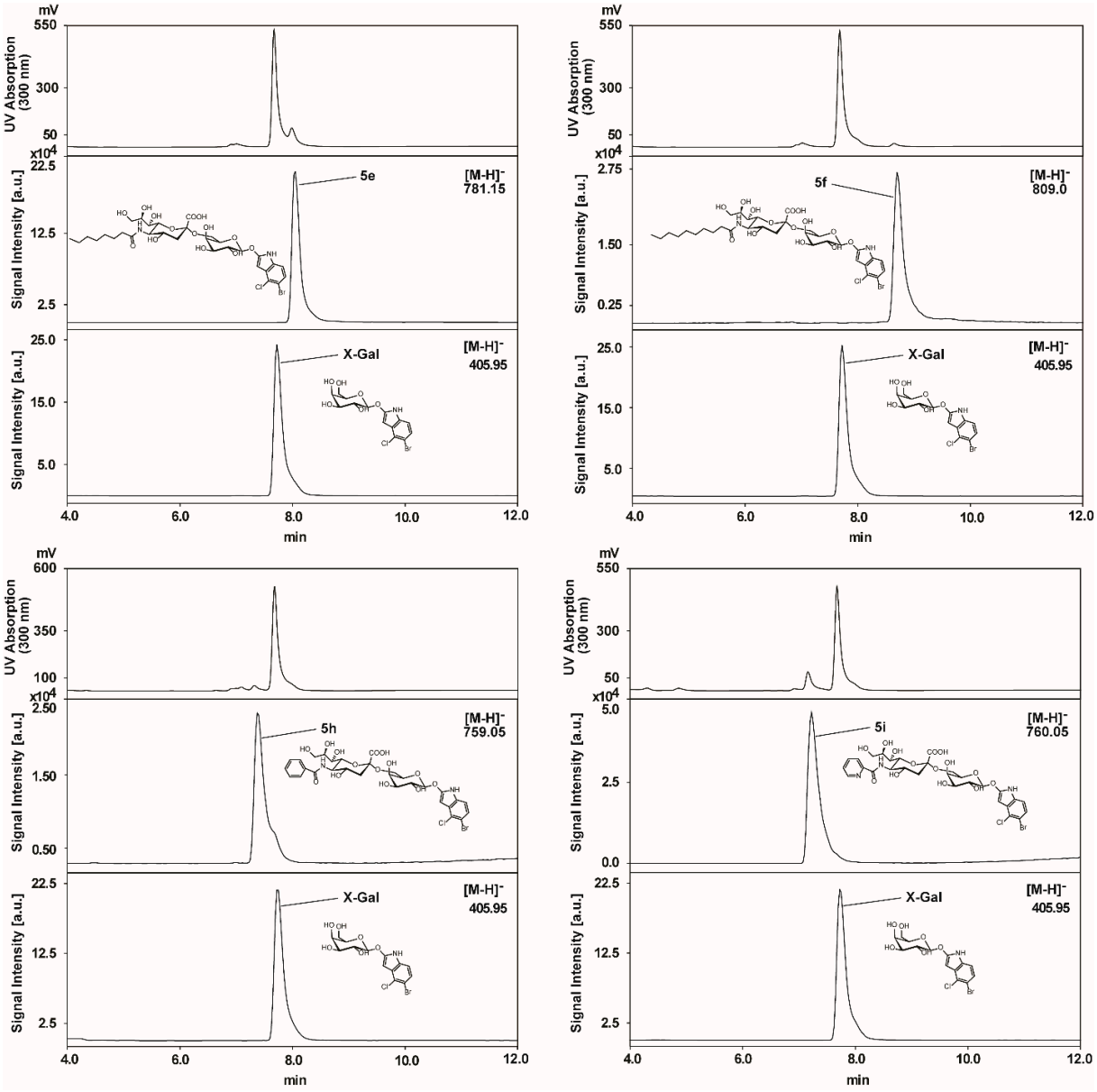

Figure S5. MS analysis of the Neu5Acα2-6GalβX analogues, **5e, 5f, 5h, 5i**, obtained by a four-enzyme, one-pot reaction using GlcNAc derivatives **1e, 1f, 1h, 1i** as the substrates.

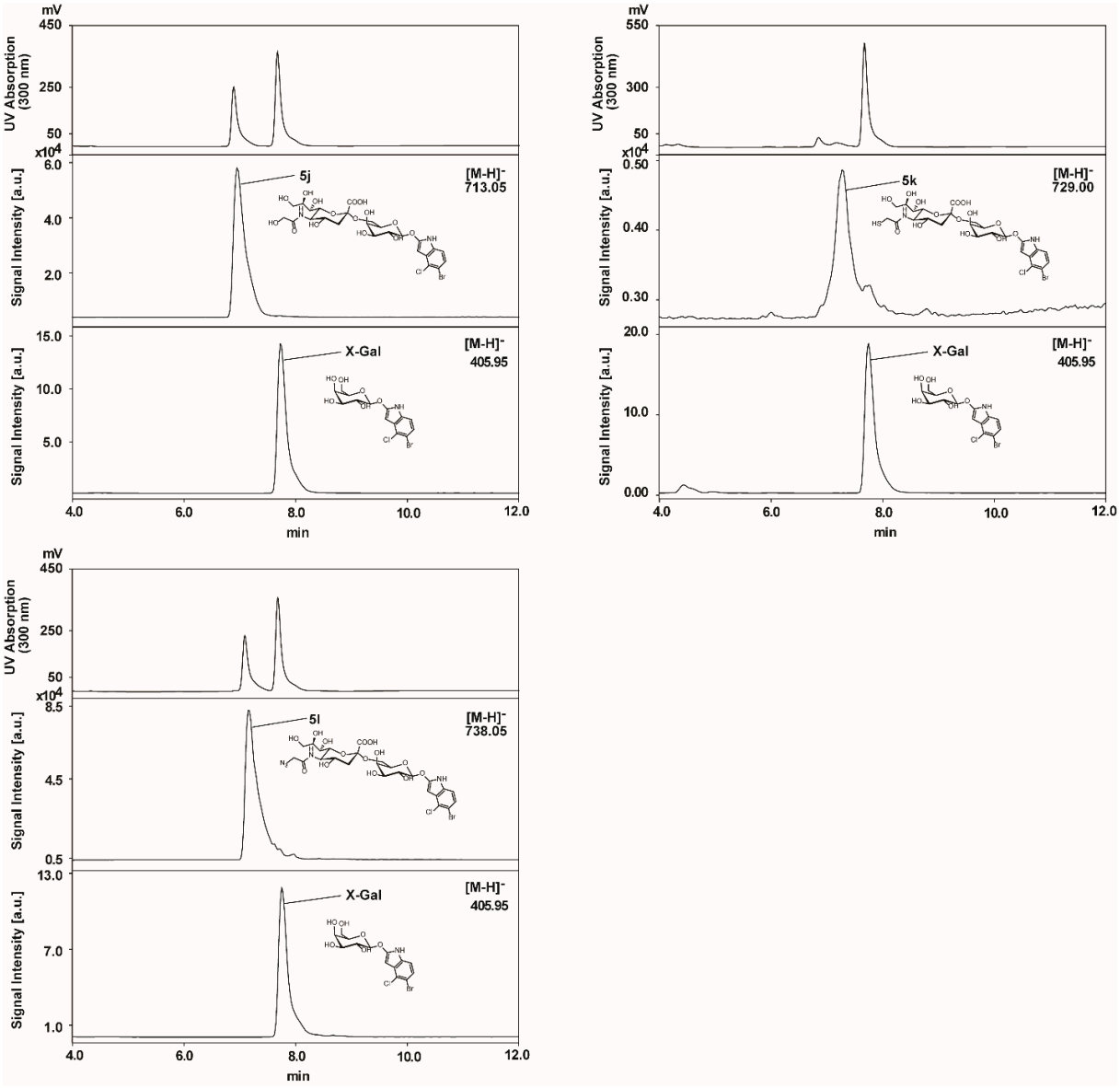

Figure S6. MS analysis of the Neu5Acα2-6GalβX analogues, **5j–l**, obtained by a four-enzyme, one-pot reaction using GlcNAc derivatives **1j–l** as the substrates.

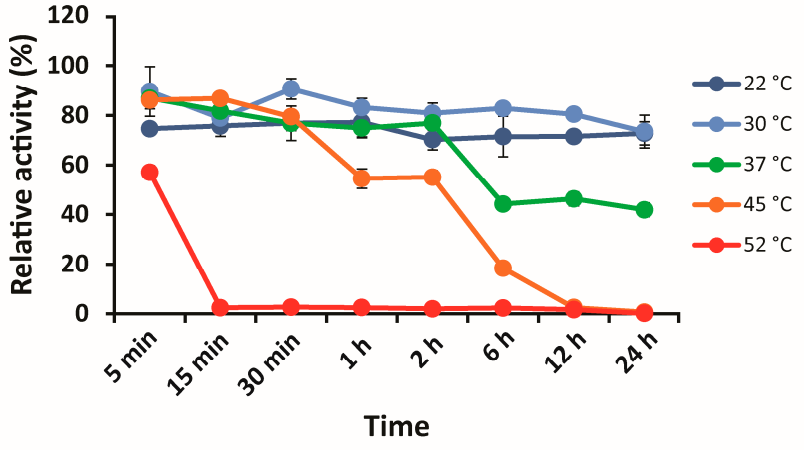

Figure S7. Relative activities of purified recombinant PhGn2E at 22 °C, 30 °C, 37 °C, 45 °C and 52 °C at different incubation time points to study the thermostability of PhGn2E. Data are presented as mean values ± standard deviation of three independent experiments.

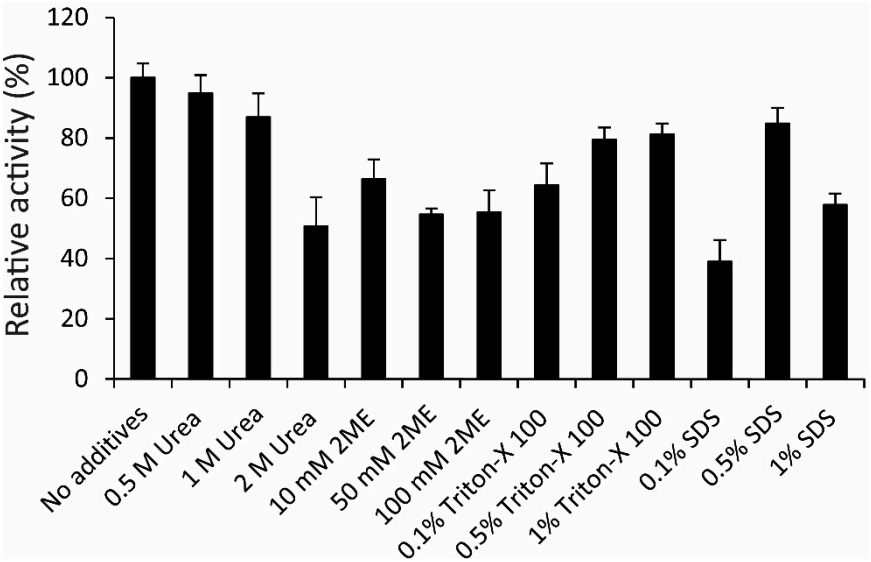

Figure S8. Relative activities of purified recombinant PhAGE in presence of different concentrations of urea, 2-mercaptoethanol (2ME), sodium dodecylsulphate (SDS) and Triton X-100. Data are presented as mean values ± standard deviation of three independent experiments. 0.5% SDS showed lower inhibition on PhGn2E compared with 0.1% and 1% SDS. As different forms of aggregation exist for SDS at different concentrations, one possible explanation could be that different aggregation stages of SDS may increase or decrease the activity of PhGn2E. For example, the critical micelle concentration (CMC), for SDS is 0.28%, which lies between the two measured concentrations of 0.1% and 0.5% SDS [1,2]. It might be that these micelles enhance the activity of PhGn2E at SDS concentrations at 0.5%, but further addition of SDS may lead to denaturation of the protein.

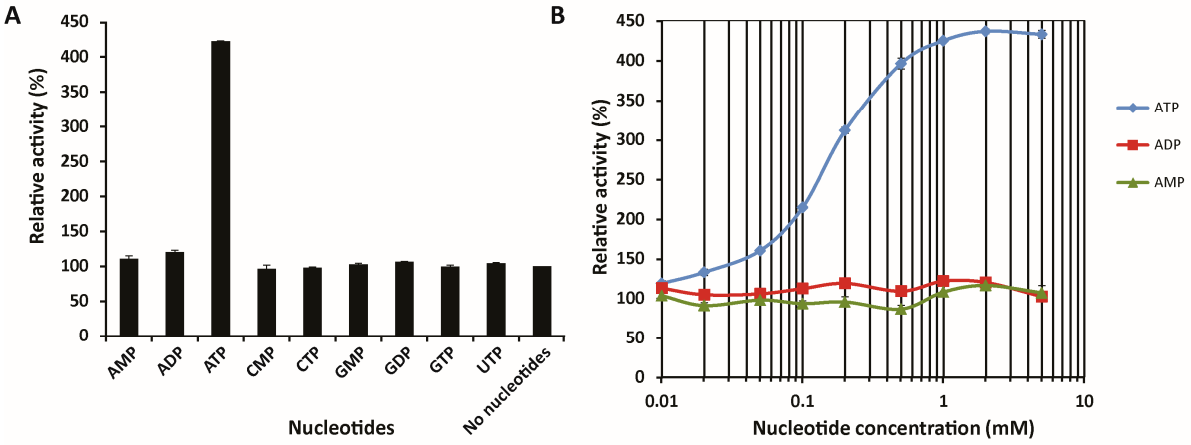

Figure S9. (**A**) Relative activities of purified recombinant PhGn2E in the presence of 2 mM of AMP, ADP, ATP, CMP, CTP, GMP, GDP, GTP and UTP. (**B**)**:** Dose-dependent effect of AMP, ADP and ATP on the PhGn2E activity. Data are presented as mean values ± standard deviation of three independent experiments.

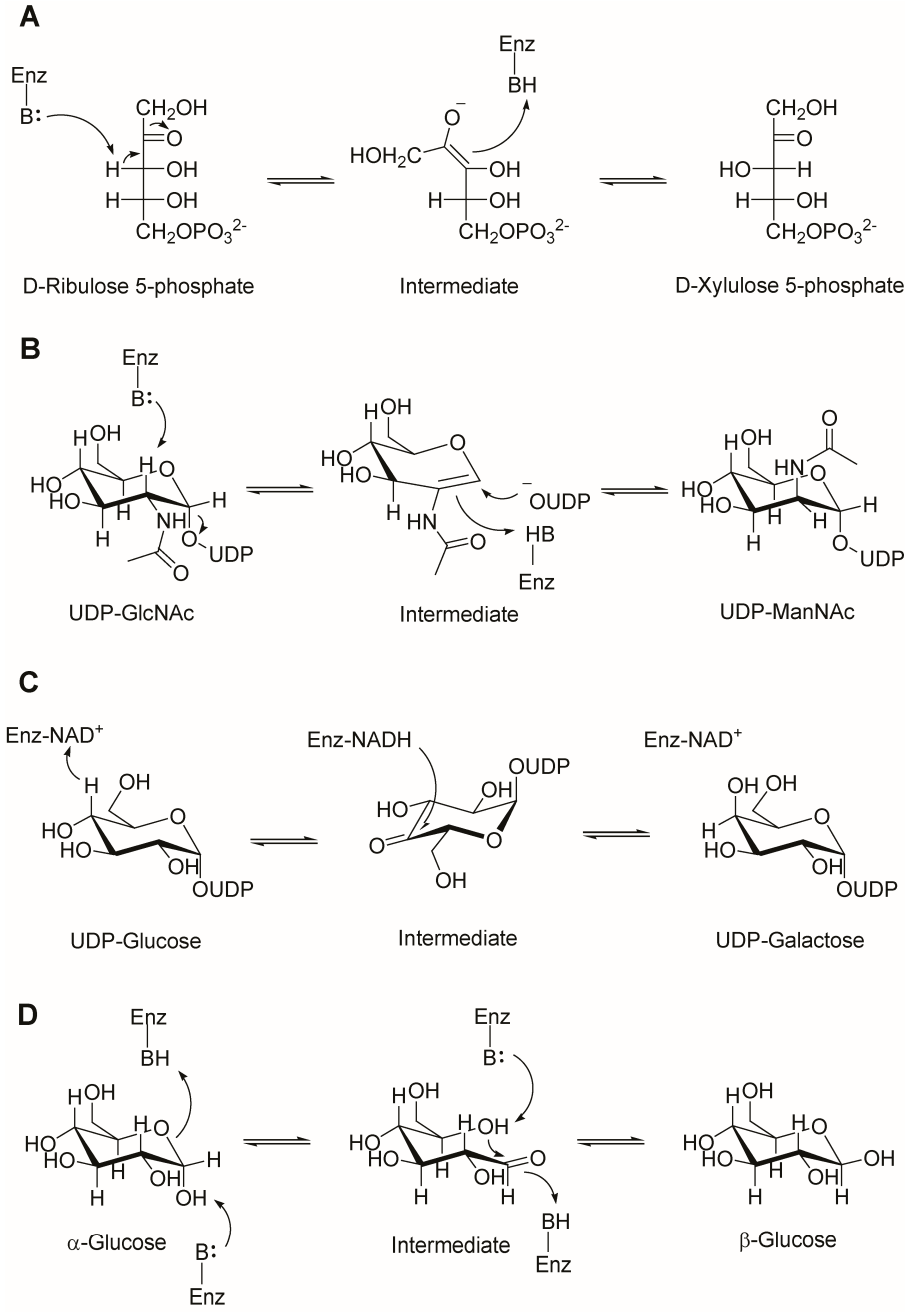

Figure S10. Examples of the different enzymatic epimerization mechanisms. **A** D-Ribulose 5-phosphate 3-epimerase—catalyze reversible conversion of D-ribulose 5-phosphate and D-xylulose 5-phosphate by deprotonation/protonation mechanism. Two residues are involved in the reaction. The intermediate anion is stablished by resonance [3]. **B** UDP-GlcNAc 2-epimerase-catalysed reversible conversion of UDP-GlcNAc and UDP-ManNAc by elimination mechanism. Two residues are involved in the reaction. The anomeric C-O of the closed ring sugar cleaves allowing the formation of the acetamido intermediate [4]. **C** UDP-galactose 4-epimerase-catalyzed reversible conversion of UDP-glucose and UDP-galactose by transient oxidation-reduction mechanism. Only one residue is involved in the reaction. The enzyme acts in a non-activated stereogenic centre [5] **D** Aldolase 1-epimerase—catalyzed reversible conversion of α-glucose and β-glucose by mutarotation mechanism. This mechanism is specific for epimerization on the anomeric carbon [6].

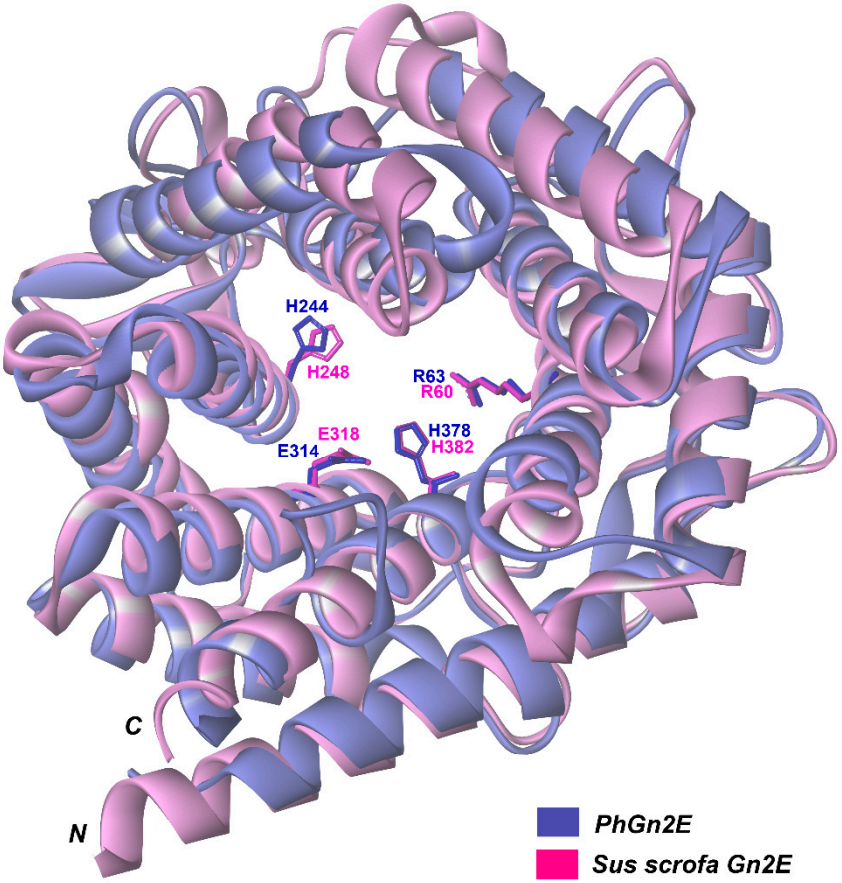

Figure S11. Structural overlay of porcine Gn2E (PDB 1fp3, pink ribbon) with the modeled PhGn2E structure (blue ribbon). Mutated amino acids R63, H244, E314 and H378 of PhGn2E and the corresponding porcine residues are displayed in blue and pink. The PhGn2E homology model was generated using the highly homologous GlcNAc 2-Epimerase from *Anabaena sp.* (PDB 2gz6) by using the MODELLER homology software (Version 9.17). The protein overlay was generated using Accelrys Discovery Studio Visualizer (Version 4.0).

Table S2. Primer sequences used to generate mutant PhGn2E variants.

Mutation	Sequence
R63A-F	5′-TAAAGCTGTATGGATACAAGGGGCTGCCGCCTGGTTGCTGTCAACTT-3′
R63A-R	5′-AAGTTGACAGCAACCAGGCGGCAGCCCCTTGTATCCATACAGCTTTA-3′
H244A-F	5′-CGTACCTTAAACCCCGGAGCTGCGATTGAAGGGGCCTGG-3′
H244A-R	5′-CCAGGCCCCTTCAATCGCAGCTCCGGGGTTTAAGGTACG-3′
E314A-F	5′-TGGCCCCATAATGCTGTCATAATCGCA-3′
E314A-R	5′-TGCGATTATGACAGCATTATGGGGCCA-3′
H378A-F	5′-AAAGGCCCTTTTGCTTTGCCAAGACAG-3′
H378A-R	5′-CTGTCTTGGCAAAGCAAAAGGGCCTTT-3′

References

1. Urum, K., Pekdemir, T., Evaluation of biosurfactants for crude oil contaminated soil washing. *Chemosphere*, **2004**, 57, 1139-1150.
2. Rahman, A., Effect of pH on the critical micelle concentration of sodium dodecyl sulphate. *J. Appl. Polym. Sci.*, **1983**, 28, 1331-1334.

3. McDonough, M. W., Wood, W. A., The mechanism of pentose phosphate isomerization and epimerization studied with T_2O and H_2O^{18}. *J. Biol. Chem.*, **1961**, 236, 1220-1224.
4. Morgan, P. M., Sala, R. F., Tanner, M. E., Eliminations in the reactions catalyzed by UDP-*N*-acetylglucosamine 2-epimerase. *J. Am. Chem. Soc.*, **1997**, 119, 10269-10277.
5. Deupree, J. D., Wood, W. A., L-Ribulose 5-Phosphate 4-Epimerase from *Aerobacter aerogenes* EVIDENCE FOR A ROLE OF DIVALENT METAL IONS IN THE EPIMERIZATION REACTION. *J. Biol. Chem.*, **1972**, 247, 3093-3097.
6. Isbell, H. S., Pigman, W. Mutarotation of Sugars in Solution: PART II: Catalytic Processes, Isotope Effects, Reaction Mechanisms, and Biochemical Aspects. *Adv. Carbohydr. Chem. Biochem.*, **1969**, 24, 13-65.